Journal of Nuclear Materials 379 (2008) 68–79

Contents lists available at ScienceDirect

Journal of Nuclear Materials

journal homepage: www.elsevier.com/locate/jnucmat

Kohonen mapping of the crack growth under fatigue loading conditions of stainless steels in BWR environments and of nickel alloys in PWR environments

Mirna Urquidi-Macdonald *

Pennsylvania State University, Department of Engineering Science and Mechanics, 203 C EES Building, University Park, PA 16802, United States

A B S T R A C T

In this study, crack growth rate data under fatigue loading conditions generated by Argonne National Laboratories and published in 2006 were analyzed [O.K. Chopra, B. Alexandreanu, E.E. Gruber, R.S. Daum, W.J. Shack, Argonne National Laboratory, NUREG CR 6891-series ANL 04/20, Crack Growth Rates of Austenitic Stainless Steel Weld Heat Affected Zone in BWR Environments, January, 2006; B. Alexandreanu, O.K. Chopra, H.M. Chung, E.E. Gruber, W.K. Soppet, R.W. Strain, W.J. Shack, Environmentally Assisted Cracking in Light Water Reactors, vol. 34 in the NUREG/CR-4667 series annual report of Argonne National Laboratory program studies for Calendar (Annual Report 2003). Manuscript Completed: May 2005, Date Published: May 2006], and reported by DoE [B. Alexandreanu, O.K. Chopra, W.J. Shack, S. Crane, H.J. Gonzalez, NRC, Crack Growth Rates and Metallographic Examinations of Alloy 600 and Alloy 82/182 from Field Components and Laboratory Materials Tested in PWR Environments, NUREG/CR-6964, May 2008]. The data collected were measured on austenitic stainless steels in BWR (boiling water reactor) environments and on nickel alloys in PWR (pressurized water reactor) environments. The data collected contained information on material composition, temperature, conductivity of the environment, oxygen concentration, irradiated sample information, weld information, electrochemical potential, load ratio, rise time, hydrogen concentration, hold time, down time, maximum stress intensity factor (K_{max}), stress intensity range (ΔK_{max}), crack length, and crack growth rates (CGR). Each position on that Kohonen map is called a cell. A Kohonen map clusters vectors of information by 'similarities.' Vectors of information were formed using the metal composition, followed by the environmental conditions used in each experiments, and finally followed by the crack growth rate (CGR) measured when a sample of pre-cracked metal is set in an environment and the sample is cyclically loaded. Accordingly, one experiment will result in a long vector of data containing information such as [Fe, wt%], [Cr,wt%], [Temperature, T], [Electrochemical potential, ECP], [K_{max}], [Conductivity, k], [CGR], etc. In that long data-vector, CGR is only one component of the vector. To 'increase' the importance of the CGR over the other components of the data-vectors, 'functional links' or functions of the CGR (as powers, logarithms, etc.) are added to each one of the vectors, resulting in longer vectors. The trained Kohonen map cells adopt 'average' values from all of the vectors stored in that cell. Accordingly, each Kohonen cell is 'represented' by and 'average' vector. The 'average' vectors representing each one of the Kohonen trained cells are topologically arranged on the map surface; i.e. 'high crack growth rates' vectors are stored on cells far apart of 'low crack growth rates' cells. Each of the parameters forming the vector can be investigated; maps of the trends of each parameter were drawn and those maps were compared to the maps of the CGRs. This paper presents the results by means of 3-dimensional figures that show the beneficial and detrimental effects that each of the variables considered has on the CGR on austenitic stainless steel weld heat affected zones in BWR environments and on nickel alloy welds in PWR environments. Data-mining methodologies (including clustering analysis) are useful to extract information from data. 'Nuclear waste' belongs to a category of subjects that are extremely complicated, mainly because many electrochemical and material-related phenomena can occur simultaneously. Stress corrosion cracking can be present among the corrosion problems faced by nuclear waste storage. The data-mining on 'the effect of material composition and environment on the CGRs' (presented in this paper – in our knowledge used by first time in the area of nuclear waste) is to be used by the reader as an example of a methodology that can be adopted for other problems encountered in the nuclear waste industry and for which data are available.

* Tel.: +1 814 863 4217; fax: +1 814 863 7967.
E-mail address: mumesm@engr.psu.edu

0022-3115/$ - see front matter © 2008 Elsevier B.V. All rights reserved.
doi:10.1016/j.jnucmat.2008.06.041

1. Introduction

1.1. The problem

Thin and long cracks formed under fatigue loading and environmental conditions are unfortunately found in the nuclear industry and they may represent a threat to the integrity of the nuclear waste isolation systems. Crack growth rate in nuclear environments is the result of a combined electrochemical and mechanical (due to the fatigue load conditions or constant load) effects. There are three principal regimes that can be recognized when the logarithm of the crack growth rate is plotted versus the electrochemical potential (ECP). Two of those regimes are dominated by the environment; they are characterized by much larger crack growth rates than if the regime was to be dominated only by the 'mechanical' regime. Those three regimes are (1) 'hydrogen embrittlement' regime, usually found at more negative ECPs on the curve Log(CGR) versus ECP; (2) 'mechanical' regime at intermediate ECP (the crack growth rates are the smallest when contrasted with the other two regimes – there is no dependency on the ECP in that regime); and (3) 'environmental' regime at more positive ECPs (the crack growth rates are controlled by diffusion of the ions formed inside the crack (due to the electrochemical crack tip dissolution (oxidation)) and reacting at the crack mouth or outside of the crack; closing the electrical circuit needed to maintain charge balance. Depending on the metal and environment of choice, one 'regime' may overrule the other 'regime.' The faster crack growth rates in nuclear reactors are observed when the 'environmental' regime overruns the 'mechanical' regime or when the 'hydrogen embrittlement' regime overruns the 'mechanical' regime [4]. The boiling water reactor coolant water chemistry operates such that the ECP is displaced below a critical value of $-0.23V_{she}$ [4]. It has shown in the past [4] that the crack that appears after many years of operation – in well-operated nuclear reactors – has an 'environmental' regime that is more important than the 'mechanical' regime or the 'hydrogen embrittlement' regime is more important than 'mechanical' regime [5].

1.2. Data

Crack growth rates were collected from tables of data published in internal reports generated by Argonne National Laboratory [1–3]. The data collected were measured on austenitic stainless steels in BWR environments and on nickel alloys in PWR environments.

Austenitic stainless steel (SS) specimens – neutron irradiated and not irradiated, and from heat affected zones (HAZ) of type 304, 304L, 316, and 316L under BWR environments – were laboratory prepared; the specimens were cut out of HAZ and weld zones from the Grand Gulf reactor core and from type 304 SS HAZ laboratory-prepared welds. The composition of the alloy SS used is shown in Table 1.

Also, crack growth tests were completed on an Alloy 600 round robin specimen and Alloy 182 weld specimen in simulated PWRs primary water at 320 °C. The CGRs obtained with a trapezoidal waveform (i.e., a constant load with periodic unload/reload, and a load ratio R, $0.21 < R < 0.71$) were comparable to the average behavior of Alloy 600 in a PWR environment. The composition of the Ni-based alloys is shown in Table 2.

Notice that when data were not available, we assumed that the weight percentile was lower than the detectable value and we set it at zero. The collected data maximums and minimums of each one of the variables considered are shown in Table 3 for BWR and in Table 4 for PWR.

Because the volume of data produced was not very large (a few hundred experiments were reported all together), the author proceeded to conduct the data analysis as follows:

(1) BWR conditions, mainly Fe-based alloys.
(2) PWR conditions, mainly Ni-based alloys.
(3) All data were assembled in a single table; data included measurements of CGR in PWR and BWR conditions, in Fe-based and Ni-based alloys.

Long vectors were formed (size 30) to represent each experiment performed. Those vectors contained the alloy composition, mechanical and environmental conditions, and crack growth rates. However, for a single reactor environment and alloy type, the number of datum vectors measured was limited (to <100 points); the results (Kohonen trained map) obtained during the clustering exercise resulted in 'noise' and the program warned the user that the number of examples was too small. Accordingly, in this paper, after analyzing the Fe alloys in BWR environments and the Ni alloys in PWRs environments, the author analyzed the data all together and performed the clustering analysis resulting when all data

Table 1
Stainless steel alloy composition used in this study [1]

Type	Heat ID	Analysis	Ni	Si	P	S	Mn	C	N	Cr	Mo	O
304	10285	Vendor	8.40	0.51	0.032	0.006	1.64	0.058	–	18.25	0.41	–
		ANL	8.45	0.60	0.015	0.007	1.90	0.070	0.084	18.56	0.51	0.013
304L	GG top shell	ANL	9.05	0.53	0.027	0.016	1.84	0.013	0.064	18.23	0.44	0.010
	GG bottom shell	ANL	8.95	0.55	0.023	0.008	1.80	0.015	0.067	18.62	0.31	0.014

Table 2
Chemical composition (wt.%) of Alloy 600 base metal and Inconel 182 and 82 weld metals [2]

Alloy ID (Heat)	Analysis	C	Mn	Fe	S	P	S i	Cu	Ni	Cr	Ti	Nb	Co
A 600 (NX1310)	Vendor	0.07	0.22	7.39	0.002	0.006	0.12	0.05	76.0	15.55	0.24	0.07	0.058
	ANL	0.07	0.22	7.73	0.001	–	0.18	0.06	75.34	16.39*	–	–	–
A 600 (NX1933)	Vendor	0.08	0.26	9.55	0.003	–	0.15	0.10	73.3	15.90	–	–	–
A 182	Spec.	0.10	5.0–9.5	6.0–10.0	0.015	–	1.0	0.5	Balance	13.00–17.00	1.0	1.00–2.50	0.12
A 182	ANL	0.05	6.97	6.82	0.005	0.008	0.56	0.01	69.22	–	–	1.70	–
A 182 Double-J	ANL	0.04	6.58	6.48	0.005	0.022	0.33	0.04	70.6	14.30	0.36	1.13	0.03
A 182 Deep Groove	ANL	0.04	7.08	6.82	0.005	0.025	0.35	0.03	70.4	13.80	0.3	1.06	0.02
A 82	Spec.	0.10	2.5–3.5	3.0	0.015	–	0.5	0.5	Balance	18.00-22.00	0.75	2.00–3.00	0.75

* Estimated as the balance. Not value was showed in original Table [2].

Table 3
Maximum and minimum values of the variables (in BWR environments) considered for training the Kohonen map [1]

	C (wt%)	Mn (wt%)	Fe (wt%)	S (wt%)	P (wt%)	Si (wt%)	Cu (wt%)	Ni (wt%)	Cr (wt%)
Maximum	0.070	1.90	69.791	0.016	0.027	0.6	0	9.05	18.62
Minimum	0.013	1.84	69.543	0.007	0.015	0.53	0	8.45	18.23

	Ti (wt%)	Nb (wt%)	Co (wt%)	Mo (wt%)	N (wt%)	O (wt%)
Maximum	0	0	0	0.51	0.084	0.014
Minimum	0	0	0	0.31	0.064	0.010

	Temperature (°C)	Test time (h)	Flow rate (cc/min)	Pt ECP mV SHE at 289 °C	Steel ECP mV SHE at 289 °C	Conductivity (μS/cm)	$[O_2]$ (ppb)	*R*, Load Ratio	Rise time (s)	Down time (s)
Maximum	289	1100	140	261	225	0.30	590	1.00	1000.00	12.00
Minimum	289	46	0	−557	−633	0.07	10	0.17	0.25	0.25

	Hold time (s)	K_{max} (MPa m^0.5)	ΔK_{max} (MPa m^0.5)	Allowed K_{max} (MPa m^0.5)	Crack length (mm (initial 6 mm)	Weld	Growth rate (m/s)
Maximum	9700	38.6	14	30.5	9.367	1	7.60E−08
Minimum	0	13.0	0	13.1	6.700	0	1.00E−14

Table 4
Maximum and minimum values of the variables (in PWR environments considered) for training the Kohonen map [2,3]

	C (wt%)	Mn (wt%)	Fe (wt%)	S (wt%)	P (wt%)	Si (wt%)	Cu (wt%)	Ni (wt%)	Cr (wt%)
Maximum	0.10	7.25	8.00	0.0150	0.006	1.00	0.500	76.0000	20.0
Minimum	0.07	0.22	3.00	0.0020	0.000	0.12	0.005	65.2650	15.0

	Ti (wt%)	Nb (wt%)	Co (wt%)	Mo (wt%)	N (wt%)	O (wt%)
Maximum	1.00	2.50	0.7500	0.0	0.0	0.0
Minimum	0.24	0.07	0.0058	0.0	0.0	0.0

	Temperature (°C)	Test time (h)	Flow rate (cc/min)	Pt ECP mV SHE at 289 °C	Metal ECP mV SHE at 289 °C	Conductivity (μS/cm)	$[O_2]$ (ppb)	*R*, Load ratio
Maximum	320	2141	50.0	−440	−434	26	9	1.0000
Minimum	316	25	0.0	−706	−704	12	9	0.2600

	Rise time (s)	Down time (s)	Hold time (s)	K_{max} (MPa m^0.5)	ΔK_{max} (MPa m^0.5)	Allowed K_{max} (MPa m^0.5)	Crack length (mm) (initial 6mm)	Weld	Growth Rate, m/s
Maximum	1000.00	500.00	3600	51.61	32.67	27.60	29.185	1.0000	7.54E−07
Minimum	0.25	0.25	0	19.40	0.00	19.10	5.993	0.0000	1.00E−14

points were used (BWR and PWR environments, and Fe-based and Ni-Based alloys).

A vector of size 30 is used to represent the alloy composition, environment, and CGRs. The author used the vectors (size 30) to train a Kohonen map. Once the map is trained, the vectors are clustered by 'similarities'. The CGRs in each map cell were plotted. The trends adopted for the CGRs were compared to the trends of each one of the component adopted by the same Kohonen map – of the vectors (size 30).

1.3. Kohonen maps

Imagine a Kohonen map as a two-dimensional array (or layer) of safe boxes. Each box or neuron can store a 'treasure.' The treasures stored are vectors of any size (in our application, of size 30) containing the information from one experiment. Kohonen maps belong to the generic Self-Organizing Maps (SOM) – defined as part of the Neural Networks family. Neural Networks are part of techniques used to mine data (data-mining). Kohonen network is one of the most fascinating topics in the neural network field. Such networks can learn to detect regularities and correlations in their input and adapt their future responses according to that input. The neurons or cells of competitive networks learn to recognize groups of similar input vectors. Self-organizing maps learn to recognize groups of similar input vectors in such a way that neurons physically near each other in the neuron layer respond to similar input vectors [6]. Self-organizing maps (SOM) learn to classify input vectors according to how they are grouped in the input space. SOM neighboring neurons in the self-organizing map learn to recognize neighboring sections of the input space. Thus, self-organizing maps learn both the distribution and topology of the input vectors on which they are trained. Given a two-dimensional map or layer of neurons, each neuron is given to store a randomly generated vector of the same size of the vectors we want to cluster. Each vector to be classified is 'presented' to the layer of neurons and compared with the stored vector contained in each neuron. The neuron that contains the vector that is most similar to the presented-to-the-net vector is declared 'the winner,' and the vector stored and its neighbor neurons are updated to make the neighborhood more similar to the vector just presented. In this way, the neighbor's neurons start to store vectors that are similar to its neighbors. Consequently, after many presentations, neighboring neurons will have learned vectors similar to each other. Scheme 1 show a hypothetical Kohonen layer formed by 9×7 cells or neurons with each neuron storing a vector $\mathbf{x}$ of size n.

Once the full layer of neurons or cells is trained, the neurons or cells that are similar cluster together, while vectors that are different cluster apart. Matlab offers a tool box in which several

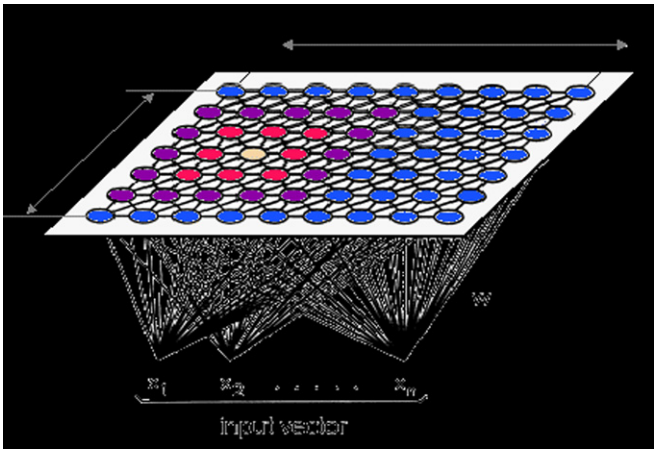

Scheme 1. Hypothetical Kohonen 9 × 7 map shows a winner neuron (3, 4) in pink and the neighborhood around the winner neuron being updated with different percentiles as color coded around the winner neuron.

functions are defined and ready to use. There are also excellent public web sites developed for gene classification that offer sophisticated Kohonen or SOM nets or engines. For example, in Matlab functions can arrange the neurons in a grid, hexagonal, or random topology. Distances between neurons are calculated from their positions with a distance function. These topology and distance functions are described in detail in Matlab or in the engine one may choose to use.

The vectors are stored by 'similarities' and topologically distributed in the two-dimensional Kohonen maps (8 cells × 5 cells); i.e., if two vectors are similar they will be stored in the same box; if two vectors are very dissimilar they will be stored far away one from the other. The trained map 'adopts' a mean value representing each one of the input vectors. A given vector is stored on the box whose adopted mean values are closest to the inputting vector. Overlapping of range of values is desirable to obtain a good result during the training. Accordingly, cells or boxes on the Kohonen map will have a mean value and a small range for each input of the vector stored. The overlapping, if it exists, is only on the neighboring cells.

In this study, an 8 × 5 Kohonen map was trained using alloy metal composition and type, parameters for PWR and BWR environmental conditions, mechanical conditions imposed on the samples, information on the origin of the samples, and measured crack growth rate. A web-based, free-to-use engine was used. Each experiment containing all the information was represented by a long vector of size 30. The size of the vector indicates the number of variables that describe an experiment; for example: C, wt%, Fe, wt%,..., K_{max}, ΔK_{max},..., T, ECP,..., CGR. While the Kohonen map is trained with the vectors for which complete data are available, the vectors are 'stored' in one of the 40 Kohonen cells or neurons (8 × 5 = 40). The position where each vector is stored does not have, *per se*, any meaning; what have meaning are how far apart the cells in the Kohonen map array are. When data that are incomplete are added to the list of vectors to be stored, that incomplete vector will be stored on the box that contains the vectors that are closer or more similar to the incomplete vector. In order to give more importance to the crack growth rate over any other variable in the vector, the author used what is called functional links. Functional links are additional inputs formed by manipulating the input considered most important to represent the classification; that is, we add inputs to each vector, information about CGR, that contain logarithm(CGR), CGR^{power} (power is any number as 2, 3, 4,...,1/2, 1/3,...).

2. Results

Before we start to show and discuss the result, the author has to keep this analysis in perspective:

(1) Results are good as the data vectors used are good.
(2) If the data used have variables that do not change, those variables will not have an impact on the results. That will not mean that variable is not important.
(3) As long we have data variability, – no matter how small is that variability – the Kohonen map will learn the information captured by that variable. All variables used were normalized to it own maximum and minimum values; accordingly, how large or how small those variables are does not matter.
(4) Data sets collected were small for BWR and PWR separately.
(5) Some variables collected are difficult to measure (example ECP); consequently, the results in the graphics are very noise and they were discarded.

Keeping these constraints in mind we will review the results.

2.1. BWR conditions, Fe-based alloys

Because the data set used – BWR and Fe-based alloys – to perform the Kohonen map training was not large enough, the Kohonen map was not well trained and the results appeared as noisy trends. The noise appeared as a rough transition from the cells of high CGRs to the cells of low CGRs.

Fig. 1 shows a three-dimensional map representation of the 'average' CGR of each one of the trained cells obtained in an 8 × 5 Kohonen map. Each cell (or neuron) stores several vectors; each cell is 'represented' by an 'average' vector. Vectors with similar values will store in the same cell, and the 'average' values are the ones that are plotted. Each one of those 'average' vectors are of size 30 (the same size of the input vectors used to train the Kohonen net). The logarithm (CGR) (an element of the vector of size 30 stored in each cell) is plotted versus the cell location in the Kohonen map. We see that for this trained Kohonen (each trained map may give different results), the only general feature is that the resultant map captures the vector information and vectors that are different will be clustered apart, while vectors that are similar will be clustered closer together in the Kohonen map. In Fig. 1, cell

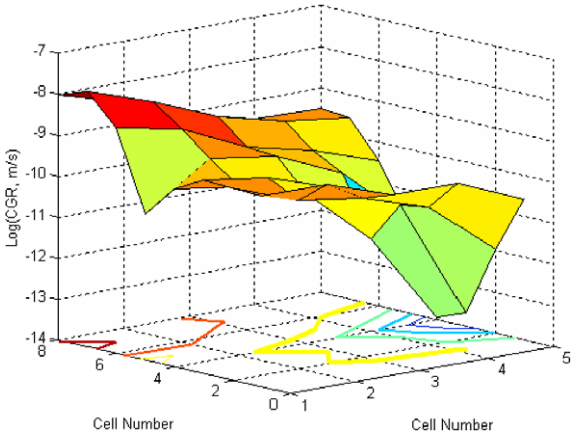

Fig. 1. Log (CGR) mean value for each trained cell (box) in the 8 × 5 Kohonen map. There is a higher CGR in cell (8,1) and lower CGR in cell (1,4). Note that when a datum vector point had an unmeasured CGR (too small to be measured); we assigned a value of 10^{-14} cm/s.

(8,1) store the vectors that have the highest CGR (average logarithm (CGR, m/s) = −8), and the lowest CGR vectors are stored in cell (1,4).

2.2. Influence of mechanical parameters

The experimental observations of the load ratio ($R = K_{min}/K_{max}$) on the CGR –of stainless steel in BWR environments – in the open literature [7] indicates that when R increased from 0.10 to 0.55, an increase in CGR was observed. This was attributed to an extrinsic effect in which crack closure was overcome. A further increase in R from 0.70 to 0.80 did not produce significant enhancement in the CGRs [7–10]. Similar results are observed in our Kohonen map clustering analysis – SSs in BWR environments – the high CGR corresponds to the low R values, and no increase in CGR is observed at high load ratios ($=K_{min}/K_{max}$). Fig. 2 shows the load ratio of the vectors stored in the different 8 × 5 Kohonen cells. As observed experimentally, it is at small load ratios that we observe the highest CGRs.

The experiments carried out by Argonne National Laboratory were CGR experiments under fatigue loading conditions that employed CT samples of SS steels (Table 1) with a given rise time, hold time, and a down time. The frequency was defined as that obtained upon the addition of all the times. Figs. 3–5 show the Kohonen cell average of the rise time, hold time and frequency. Note that for this trained Kohonen map the highest CGRs were stored in cell (8,1) and the lowest CGRs were stored in cell (1,4).

For crack with a large mouth-length/crack-length ratios, it is expected that at low applied mechanical load frequencies, the crack will remain open a longer time and – if the 'environmental' regime overruns the 'mechanical' regime – the CGR will be faster; high down-times, high hold-times and low frequencies will cluster on the Kohonen cell corresponding to the high CGRs. On the contrary, if the 'mechanical' regime overruns the 'environmental' regime, low down-times (Fig. 3), low hold-times (Fig. 4) and high frequencies (Fig. 5) will cluster with the high crack growth rates (cell (8,1)). The results, on SSs submerged in BWR environments, demonstrate that the experiments were carried out under the 'mechanical' regime; that is, it is the 'mechanical' regime that dominates the experiments carried out rather than the 'environmental' regimes. These results may explain the lack of correlation between the ECP and CGRs observed in the data. Note in Fig. 5 that high frequencies (0.8 Hz) correspond to higher CGRs while low frequencies correspond to low CGRs in this analysis.

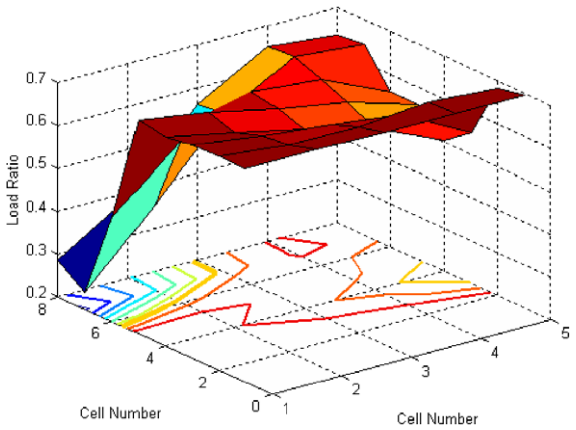

Fig. 2. Load ratio mean value for each trained cell (box) in the 8 × 5 Kohonen map. Low load ratio corresponds to high CGRs (cell (8,1), which appears to indicate that the SS has a different impact depending of the type of material, as was expected. If the alloy types are classified by their CGR, a Kohonen cell contains an average of the vectors stored in that box or cell.

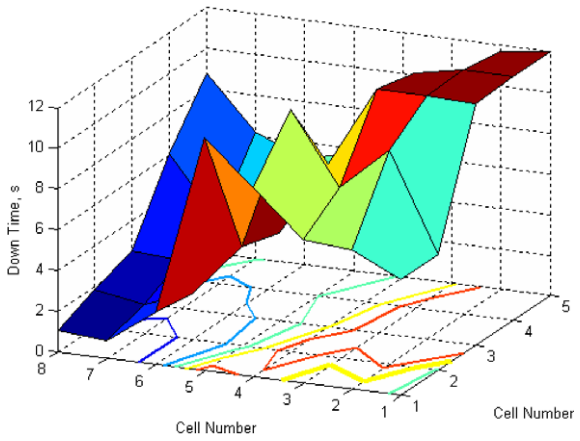

Fig. 3. Down time mean value for each trained cell in the 8 × 5 Kohonen map; higher CGR is in cell (8,1), lower CGR in cell (1,4).

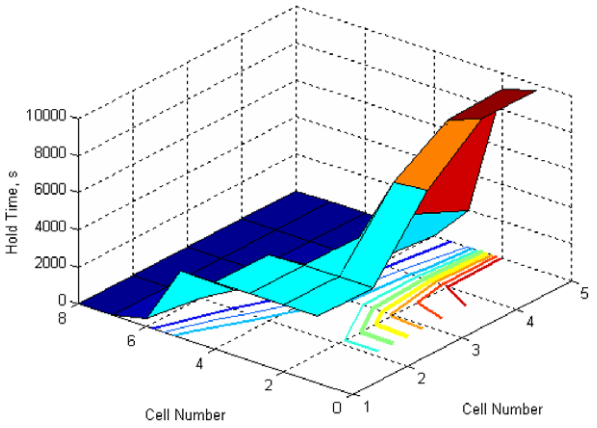

Fig. 4. Hold time mean value for each trained cell (box) in the 8 × 5 Kohonen map; higher CGR is in cell (8,1), lower CGR in cell (1,4).

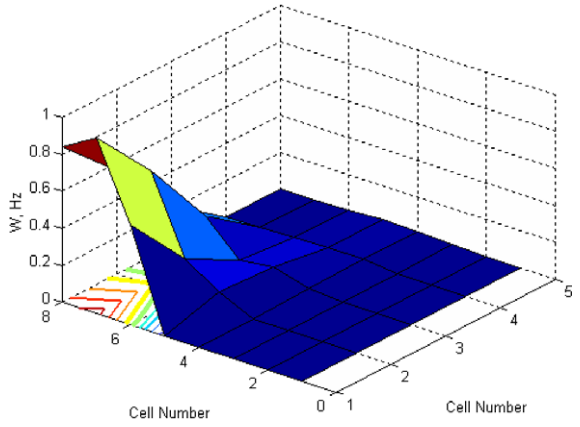

Fig. 5. Frequency mean value of each trained cell (box) in the 8 × 5 Kohonen map. High frequency corresponds to high CGRs.

Fig. 6 shows the stress intensity range (ΔK_{max}) distribution values in the Kohonen map. Larger ΔK_{max} correspond to map position (8,1), where the highest CGR values are stored (Fig. 1). These results confirm that the data analyzed and collected on SS in BWRs

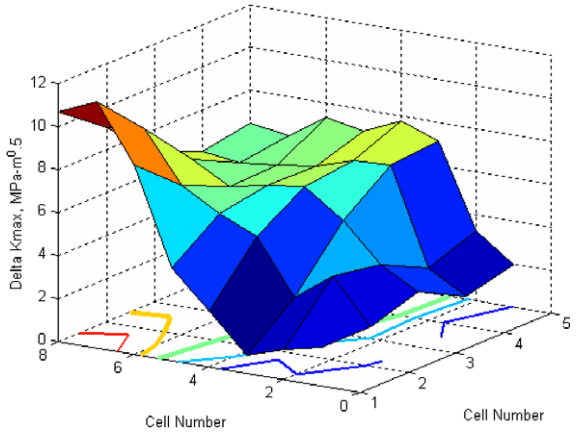

Fig. 6. Delta stress intensity factor (cyclic load; ΔK corresponds to the 'load amplitude') value of each trained cell (box) in the 8×5 Kohonen map. High delta stress intensity factor corresponds to high CGRs.

environments were collected under the 'mechanical regime' for which the smaller CGRs are observed [4,5].

2.3. Influence of environmental parameters

The most important environmental parameter in stress corrosion cracking (SCC) is claimed to be the ECP [4]. Models have shown that the sensitized Type 304 SS will suffer SCC only at ECPs above some critical **e**nvironmental assisted **s**tress **c**orrosion **c**racking (ESCC). Macdonald's model [4] showed that the CGR in sensitized Type 304 SS at ECP > ESCC increases strongly with increasing corrosion potential, probably due to an enhanced ability of the external surfaces to consume a charge emanating from the crack through the reduction of oxygen and hydrogen peroxide – radiolysis products in nuclear reactors. For ECP > ESCC the curve Log(CGR) versus ECP corresponds to the 'electrochemical oxidation (dissolution) of the crack tip' regime. The statistical analysis of the data used in this analysis – SSs on BWR environments- showed a strong correlation between the 'mechanical' regime parameters (K_{max}, ΔK_{max}, and ω) and the CGRs and a poor or non-existent correlation between the parameters that are important to describe the electrochemical or 'environmental' effects –as electrochemical potential, temperature, and conductivity – and the CGRs. Probably, this is one of the reasons why CGRs reported are smaller than the CGR measured by Argonne National Laboratories (ANL) in PWRs environments. The results obtained by analyzing the present data reflect that the 'mechanical' regime is more important than the 'environmental' regime. Noticed that the higher crack growth rates measured (on the data used) were lower than 10^{-8} m/s; which support the hypothesis that the experiment were run under 'mechanical' regimes [4].

Temperature results are not shown because the data did not contained a variation on that variable; accordingly, the learning from those variables is very insignificant.

It is important to understand that not finding relationship between a variable and CGRs does not mean that that variable is not important, but it may mean that those variables were kept constant over all the experimental data accumulated.

Based on this analysis it was concluded that these data are representative mainly (if not entirely) of the 'mechanical' effect and not the 'environmental' effect. The ECP data measured – on the metal alloy and on a platinum reference electrode – do not show any correlation with the CGRs measured. This may indicate that (a) the ECP was measured incorrectly; or (b) the regime under which the CGR was measured is overwhelmed by the 'mechanical' regime of the measured CGRs, not showing any correlation between ECP and CGRs.

2.4. PWR conditions, Ni-based alloys

The author analyzed the ANL data collected on nickel-based alloys under PWR environments. The composition of the alloys analyzed is listed in Table 2. Fig. 7 shows the results obtained on the trained Kohonen map of the logarithm (CGR). The left front side of the Kohonen map (cells (8,1) through (1,1)) stores the elements with smaller crack growth rates, where the upper-right far side (cell (8,5)) stores the vectors with the highest CGR.

Accordingly, if we plot each one of the inputs (not all inputs are plotted) in the Kohonen map, the cells (8,1) through (1,1) in this trained Kohonen map store the vectors (size 30) that are 'beneficial' in order to keep a low CGR, while the vectors stored in cells (8,5) through (1,5) are 'detrimental' to the metal (high CGRs).

2.5. Influence of alloy composition

We explore, for example, the role of minor alloy elements in the nickel based alloys; as the effect of phosphorus (Fig. 8) in the alloys used (A182, A82, A600), and find that in order to maintain low CGR we should keep the amount of phosphorus low in the nickel-based alloys.

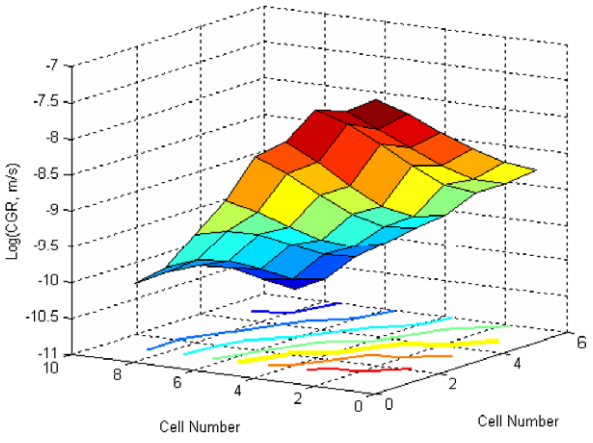

Fig. 7. Log (CGR) mean value for each trained cell (box) in the 8×5 Kohonen map; higher CGR in cell (8,1), lower CGR in cell (8,4).

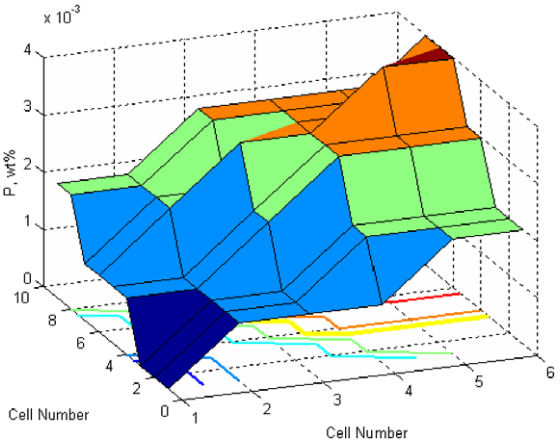

Fig. 8. Phosphorus wt% mean value for each trained cell (box) in the 8×5 Kohonen map. Low concentration of P corresponds to low CGRs (see Fig. 7).

Similar inspections on the Kohonen map can be performed for each of the alloy's elements. We find (not shown) that increasing the iron content as a minor alloy element increases the CGRs; increasing the nickel content (or lowering the total weight of the minor alloy elements such on the Ni-based alloys) increases the CGR (Fig. 9). In other words, some of the minor alloys elements in the nickel alloys are beneficial.

Fig. 10 shows that Silicon has a very small or negligible impact (on the weight percentile explored) as believed by other authors [11].

Niobium (Nb) has also a small impact on the CGR. Fig. 11 indicates that low concentrations of Nb correspond to high CGRs.

2.6. Influence of the environment

Examples of the environmental impacts on the CGR are shown in Figs. 12 and 13. Fig. 12 shows that high electrolyte flow rates correspond to high CGRs. It is reported in the literature [12] that under the 'environmental' regime (usually observed in BWRs) an increase in the flow rate increases the CGR because it increases the cathodic reaction area that occurs at the crack mouth and outside of the crack mouth side. It is important to mention that this last phrase is applicable for cracks for with the ratio between the crack's-mouth-dimension/crack-length $\gg 1$. Thin and long cracks are the most dangerous on nuclear reactors than large open cavities; because they are much difficult to detect. Large mouth cracks (as large cavities) usually develop at low flow rates. For the large mouth cracks, low flow velocities keep the aggressive environments in the crack tips; while high electrolyte floe velocities 'wash out' the crack tips becoming beneficial to the CGRs of those cracks.

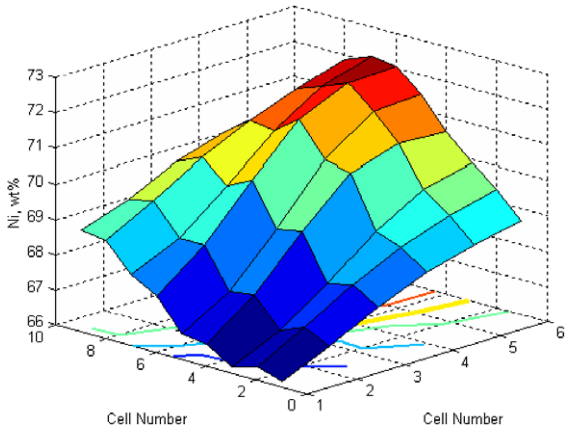

Fig. 9. Ni wt% mean value for each trained cell (box) in the 8×5 Kohonen map. High nickel content – corresponding to low content of minor alloy elements – corresponds to high CGRs.

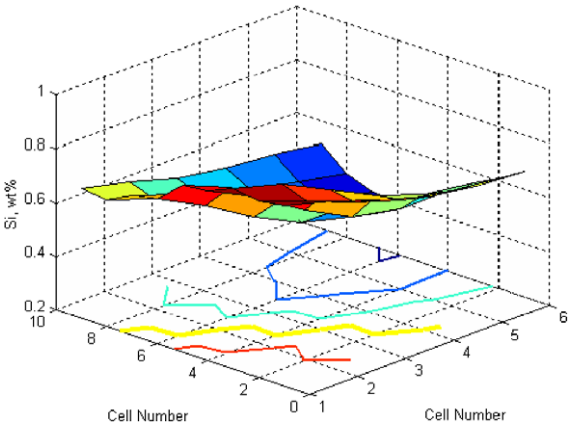

Fig. 10. Si weight percentile content has a negligible impact on CGRs for the nickel-based alloys in PWR environments.

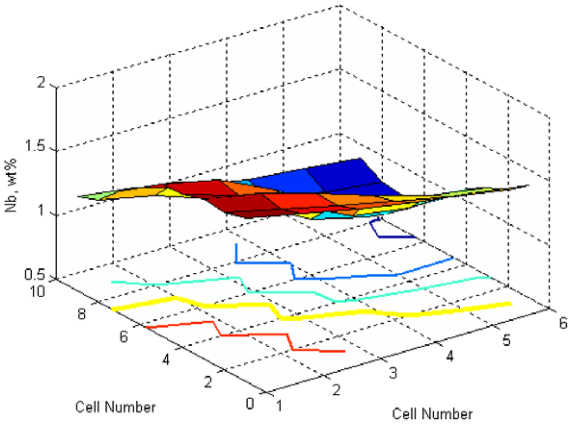

Fig. 11. Nb weight percentile content has a small impact on CGRs for the nickel-based alloys in PWR environments. Low concentrations of Nb correspond to high CGRs.

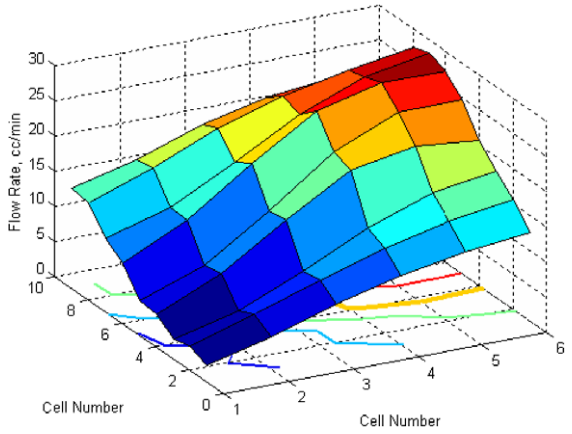

Fig. 12. Flow rate mean value for each trained cell (box) in the 8×5 Kohonen map. High flow rates correspond to high CGRs.

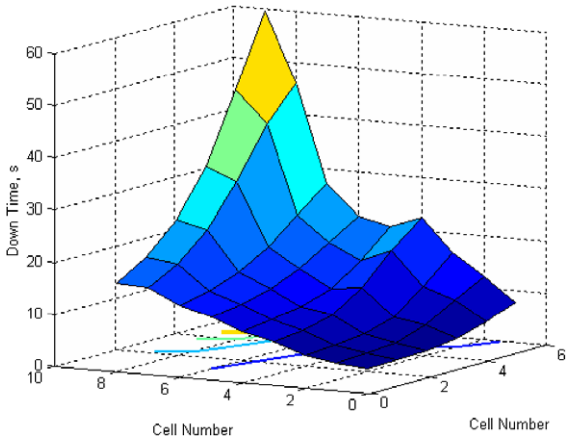

Fig. 13. Down time mean value for each trained cell (box) in the 8×5 Kohonen map. High down time corresponds to high CGRs.

In this paper, when we refer to the CGRs we refer to cracks that have a very high slender ratio (small mouth compared to the crack length).

2.7. Influence of the mechanical loads

Fig. 13 shows the mean down time of the Kohonen cells versus position on the two-dimension Kohonen map. The down time and rise time (the latter not shown) are observed to increase the CGRs when the system is in the 'environmental' regime, and the opposite is observed when the CGR is mechanically controlled [4,5,13].

The results (Figs. 12 and 13) obtained under PWR conditions on the nickel-based alloys indicate that the CGR data measured have a stronger 'environmental' regime component than the data collected for BWR conditions on Fe-based alloys.

2.8. Clustering using all data available (BWR and Fe-based, PWR and Ni-based alloys)

Because not enough data were available when the data were separated in Fe-based BWR environments and in nickel-based PWR environments, the two data sets were combined and analyzed as a whole. The results are discussed herein.

It is interesting to notice that the two previous analysis indicated that the data measured by ANL in BWR conditions was generated with a dominant 'mechanical' regime component; while the results obtained with the data measured in PWR conditions indicates that the 'environmental' regime was more important than the 'mechanical environment. Those results are supported by the high CGRs measures in PWR environment when compared to the CGRs obtained in BWR environment (see Tables 3 and 4).

It is well understood that the mechanisms that yield to CGRs in BWR environment are very different to the mechanisms that yield to CGRs in PWR environments. However, we are not sorting out here the mechanism causing CGR. We are solely mining the data expecting to learn something that we do not know and that is embodied on the measured data. By analyzing the two data sets together we loose the capability to differentiate the root of possible important mechanism that set the differences on CGRs when different metal alloys and environments are used. We hope to learn if they are minor alloy element common to both Fe- and Ni-based alloys that can be considered beneficial or detrimental to CGRs.

Fig. 14 shows the results obtained on the trained Kohonen map of the logarithm of the crack growth rate. The left front side of the Kohonen map – about cell (8,1) – stores the elements with smaller crack growth rates, while the upper-right far side – about cell (1,5) – stores the vectors with the highest CGRs. Accordingly, if we now plot each one of the inputs (not all inputs are plotted) in the Kohonen map, the same cells will indicate what is beneficial or what is detrimental to the CGR.

2.9. Minor alloy element impact on CGR

The impact of each of the minor alloys in the Ni-based and Fe-based metal alloys studied was reviewed. It is important to remember that some of the elements contained in the Ni-based alloys are not contained in the Fe-based alloys, and vice versa. Once the Kohonen map is trained, each cell assumes an 'average' vector, with each element of that 'average' vector representing each cell or neuron value storage vector. The vectors stored have exactly the same dimensions of the input vectors used in the training. Notice that the same map stores the high CGRs in cell (1,5) and the low CGRs in cell (8,1). Not surprisingly, as we will observe in the following figures, Kohonen cell (8,1) store SS alloys used in BWR environments while cell (1,5) store vectors corresponding to the Nickel alloys in PWR environments. Noticed that not all minor alloy elements analyzed are shown to avoid a very long paper.

Figs. 15 and 16 show the concentration of the Fe contents and the nickel contents of the vectors stored in the Kohonen cells. From these two figures it is clear that the Fe-based alloys are stored in the cells that contain low CGRs, while the nickel-based alloys are stored in the cells corresponding to the high CGRs. As mentioned above (BWR and PWR analysis), the data collected on the Fe-based alloys in BWR environments correspond to the 'mechanical' regime; the nickel-based alloys in the PWR environments exhibited a more prominent 'environmental' component. The ECP of the experiments carried out on the Fe-based samples in BWR environments corresponds to the range of values found in the 'mechanical' regime, while for the Ni-based alloys in the PWR environments the ECP corresponds to the 'environmental' controlled ECPs. These two previous observations are confirmed in the results depicted in Figs. 15 and 16. The Fe-based BWR environment samples correspond to lower CGRs cells (cell (8,1); while Ni-based PWR condition tested samples are stored on the Kohonen cell (1,5).

Once we identified that the high CGR stored in the Kohonen map are vectors corresponding to PWRs environments (dominated by 'environmental' regimes as indicated in the PWR data analysis in the previous section); and the low CGR correspond to vectors representing BWR environments under 'mechanical' regime (as indicated in the previous section on BWRs results) we proceed to investigate the general effect of the minor alloy elements.

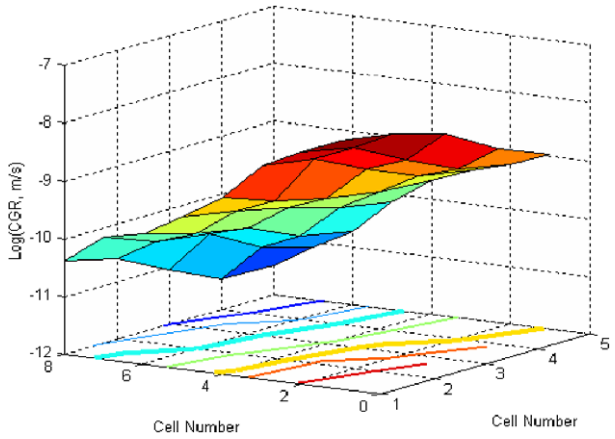

Fig. 14. Log (CGR) mean value for each trained cell (box) in the 8 × 5 Kohonen map. Lower CGR is found in cell (8,1), higher CGR in cell (1,5).

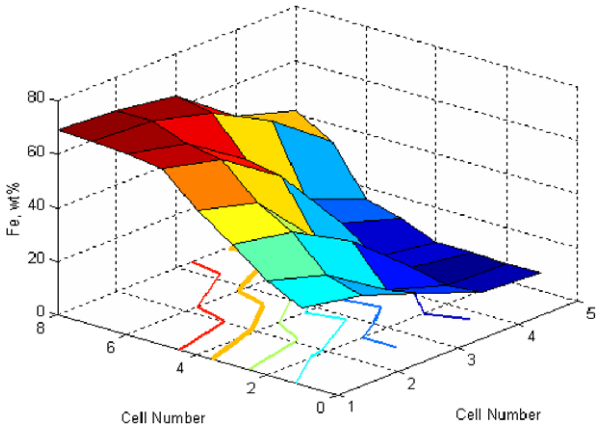

Fig. 15. Iron wt% mean value for each trained cell (box) in the 8 × 5 Kohonen map. The high CGRs (cell (1,5) correspond to the Ni-based alloys in PWR environments.

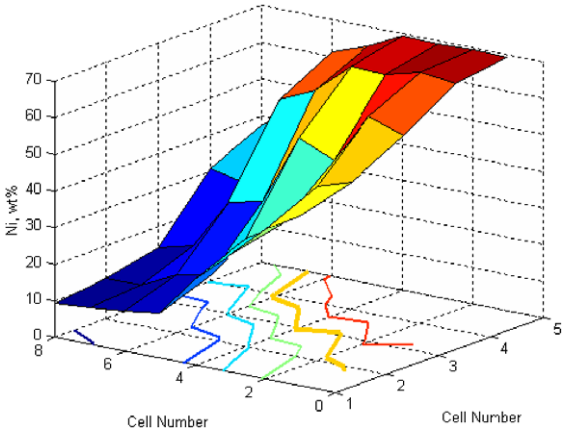

Fig. 16. Nickel wt% mean values for each trained cell (box) in the 8 × 5 Kohonen map. The high CGRs (cell (1,5) correspond to the Ni-based alloys in PWR environments. These results are consistent with the results presented in Fig. 15.

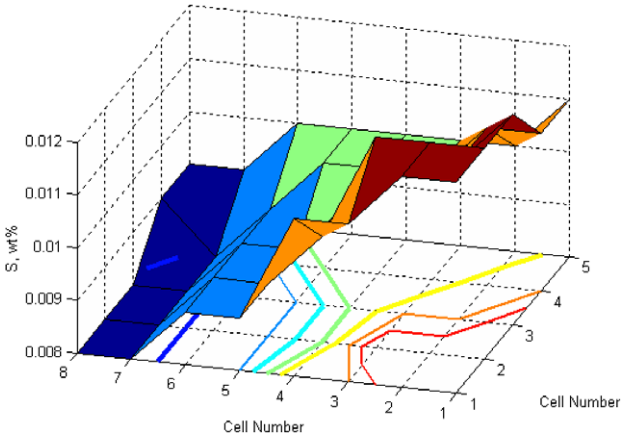

Fig. 18. Sulfur wt% mean value for each trained cell (box) in the 8 × 5 Kohonen map. If sulfur content is less than 0.008 wt%, the crack growth rates are slower.

Fig. 17 shows that the phosphorus content. The Kohonen map shows lower CGR for the Fe-based alloys with a highest [P] concentration, and in the Kohonen cell with the lowest CGRs, the Ni-based alloys show a lowest [P] concentration. These results may indicate that higher [P] concentrations were found on the Fe-based alloys and lower [P] concentrations were found on the Ni-based alloys.

Sulfur is presented in Fe-based and Ni-based alloys in concentrations of $0.007 < [S, wt\%] < 0.016$; and $0.002 < [S, wt\%] < 0.15$, respectively. Lower concentrations of [S] on Fe-alloys yield lower CGRs; higher concentrations of [S] on Ni-alloys yield to higher CGRs as shown in Fig. 18.

Similar trends are observed in Fig. 19 where the carbon wt% concentrations are clustered in the Kohonen map. Fe-based alloys that cluster on cell (8,1) have concentrations oscillating between $0.013 < [C, wt\%] < 0.07$; the best performing Fe-based alloys are alloys containing [C] = 0.04%, no more, no less. Ni-based alloy concentrations have a total concentration oscillating between $0.07 < [C, wt\%] < 0.1$. Concentrations of 0.04 wt% carbon appear to be optimal on the Fe-based alloys, while larger concentrations [C] = 0.09 wt%) on the Ni-based alloys are detrimental.

Fe-alloys do not contain copper. The Ni-based alloys with lower [Cu, wt%] cluster away from cell (1,5) where the highest CGRs occur ($0.005 < [Cu, wt\%] < 0.5$ are the concentrations on the alloy tested). Accordingly, a high concentration of copper ([Cu] =

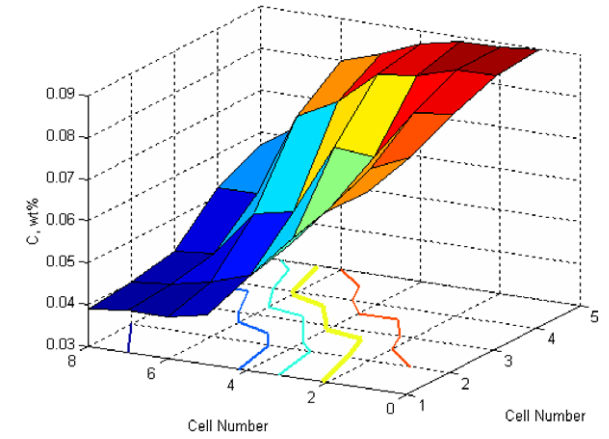

Fig. 19. Carbon wt% mean value for each trained cell (box) in the 8 × 5 Kohonen map. If carbon wt% is about 0.04, the CGRs are smaller.

0.33 wt%) in Ni-based alloys is detrimental to CGR, as shown in Fig. 20.

Chromium concentration varies between $15 < [Cr, wt\%] < 20$ in the Ni-based alloys, while concentrations of $18.23 < [Cr,$

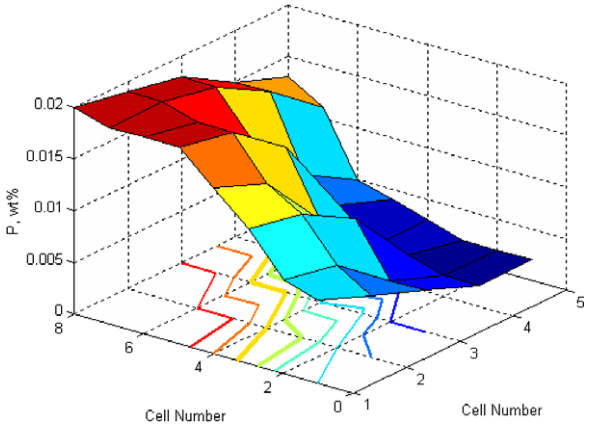

Fig. 17. Phosphorous mean value for each trained cell (box) in the 8 × 5 Kohonen map. If P = 0.02 wt%, the CGRs are slower. Fe-based alloys clustered in cells around (8,1) correspond to the best performing Fe-based alloys (lower CGRs).

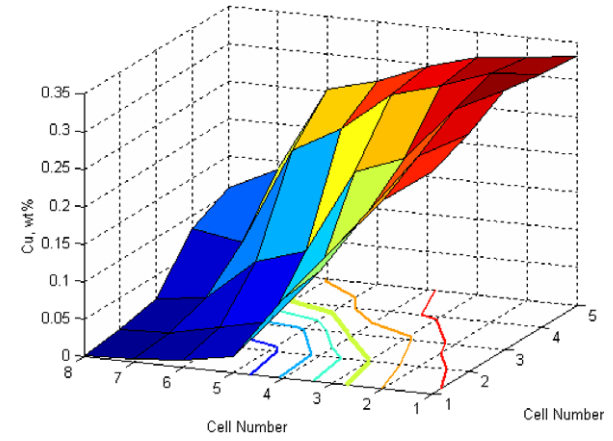

Fig. 20. Copper wt% mean value for each trained cell (box) in the 8 × 5 Kohonen map. Copper, a minor component of the alloy, was present in only a few of the alloys tested: A182, A82, and A600.

wt%] < 18.62 are present in the Fe-based alloys. Chromium content on the cluster with lowest CGR corresponding to the Fe-based alloys with concentration averages 18.55%; we can conclude that these high Cr concentrations on the Fe-based alloys are beneficial. The worse CGRs are on the Kohonen cell with the Ni-based alloys with lower chromium concentrations; we can conclude that higher chromium concentrations are beneficial in Fe- and Ni-based alloys when in the presence of BWR and PWR environments, as shown in Fig. 21.

Silicon, a minor alloy component, appears not to have an impact on increasing or decreasing the CGR in the range of concentration used (0.4–0.8 wt%) in the Fe-based and Ni-based alloys, as shown in Fig. 22.

The Fe-based alloys studied had weight percentile concentrations of Manganese in the range of 1.84 < [Mn, wt%] < 1.9, and for the Ni-based alloy the concentrations were between 0.22 < [Mn, wt%] < 7.25. The Fe-based alloys clustered on the cell with the lowest CGRs are an example with a higher Mn content. The vectors clustered in the cell with the highest CGRs correspond to the cluster containing Ni-based alloys with the largest concentration of Mn. Accordingly, while concentrations of 1.90 Mn wt% are beneficial in Fe-based alloys, large concentrations (average ~4 wt%) of Mn on Ni-based alloys are not beneficial, as shown in Fig. 23.

The Fe-based alloys contained molybdenum, N, and O as minor alloy elements in concentrations between 0.31 < [Mo, wt%] < 0.51, 0.064 < [N, wt%] < 0.084, and 0.01 < [O, wt%] < 0.014. The average

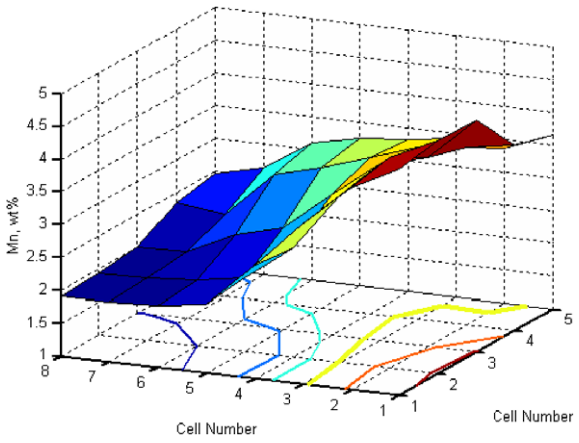

Fig. 23. Manganese wt% mean value for each trained cell (box) in the 8 × 5 Kohonen map. If Manganese, a minor alloy component, has wt% < 2, CGR is slower.

concentrations of the Mo, N, and O of the vectors stored in the Kohonen cell with the lowest CGRs are about 0.4, 0.75, and 0.013, respectively, as shown in through Figs. 24–26. Indicating that the higher concentration of O and N as a minor alloy elements, and intermediate values of the concentration of Mo are beneficial in CGRs for the Fe-based alloys in contact with a BWR environ-

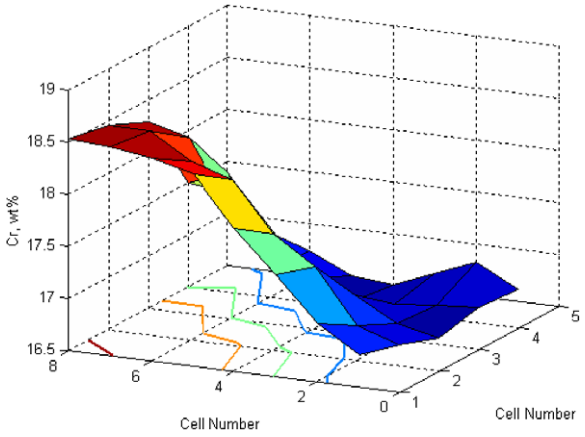

Fig. 21. Chromium wt% mean value for each trained cell (box) in the Kohonen 8 × 5 map. Higher chromium content is beneficial to slow CGR.

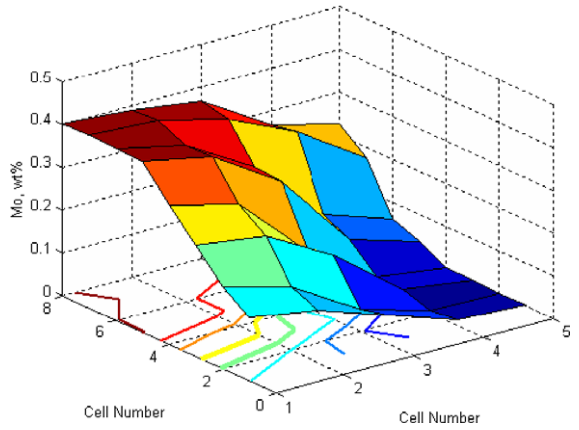

Fig. 24. Molybdenum wt% mean value for each trained cell (box) in the 8 × 5 Kohonen map. Contents of 0.4 wt% of cobalt are favorable to decrease CGR.

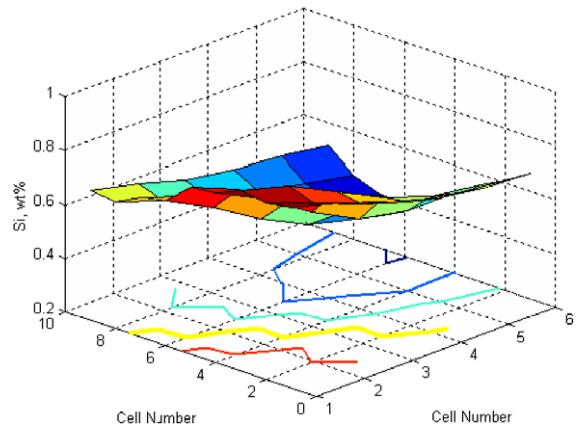

Fig. 22. Silicon wt% mean value for each trained cell (box) in the 8 × 5 Kohonen map.

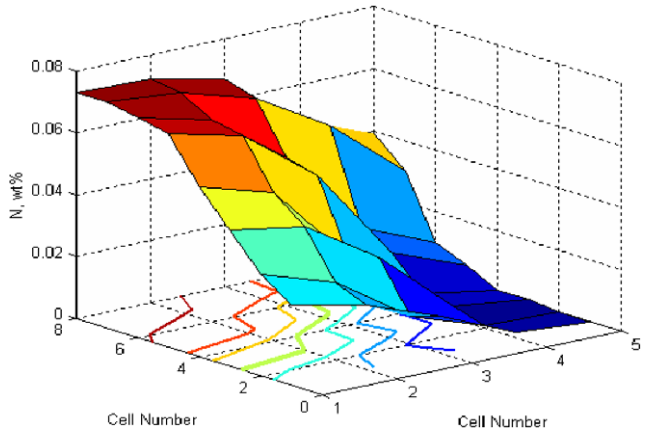

Fig. 25. Nitrogen mean value for each trained cell (box) in the 8 × 5 Kohonen map. About 0.07 wt% traces of nitrogen are favorable to decrease CGR.

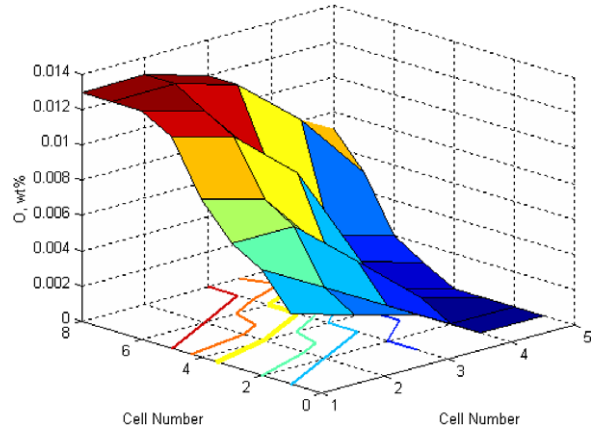

Fig. 26. Atomic oxygen wt% mean value for each trained cell (box) in the 8 × 5 Kohonen map. About 0.013 wt% traces of nitrogen are favorable to decrease CGR.

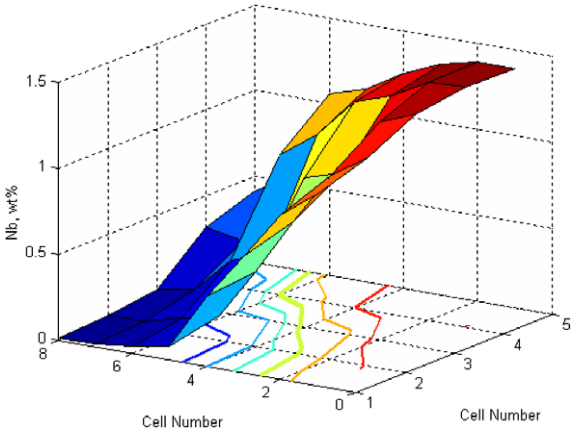

Fig. 28. Niobium wt% mean value for each trained cell (box) in the 8 × 5 Kohonen map. Niobium traces in Fe- and Ni-based alloys used in nuclear environments are detrimental to crack growth under fatigue conditions.

ment. Ni-based alloys do not contain Mo, N, or O as minor alloy elements.

Ni-based alloys contain Ti, Nb, and Co in the ranges of 0.24 < [Ti, wt%] < 1.00, 0.07 < [Nb, wt%] < 2.50, 0.0058 < [Co, wt%] < 0.75 in the alloys studied in a PWR environment. Figs. 27–29 present the averages values of Ti, Ni, and Co in the Kohonen cells that show the highest CGRs. Those values are ~0.68, 1, 45, 0.38 wt% for the Ti, Nb, and Co, respectively (as shown in Figs. 27–29). Accordingly, high concentrations of Ti and intermediate to high concentrations of Nb and Co are detrimental for the Ni-based alloys.

After exploring the impact of the alloy compositions on the CGR, the author directed her attention to the environmental parameters and the mechanical parameters that were imposed on the pre-cracked sample, exploring the effects of conductivity and temperature on the CGRs.

2.10. Environment influence

It is expected that conductivity will have a similar impact in BWRs and PWRs, in Fe-based alloys and in Ni-based alloys. The effect of conductivity was explored when the two data sets were used together to train a Kohonen map. Fig. 30 shows the effect of conductivity on CGRs. As indicated by Macdonald [4,12,14], for CGRs dominated by the 'environmental' regime, it is expected that the CGRs increases with electrolyte conductivity; because, the throwing power of the current coming out of the crack tip (due

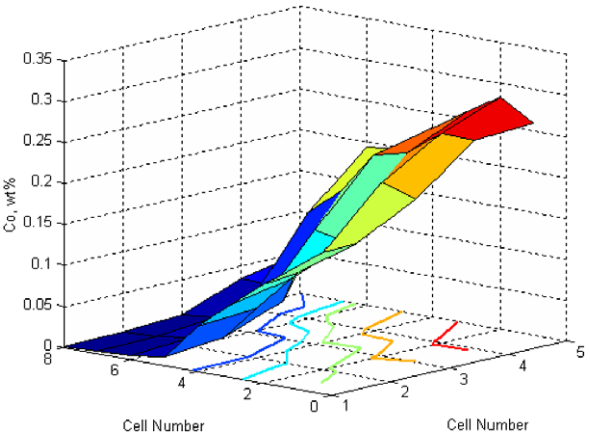

Fig. 29. Cobalt wt% mean value for each trained cell (box) in the 8 × 5 Kohonen map. Cobalt traces in Fe- and Ni-based alloys used in nuclear environments are detrimental to crack growth under fatigue conditions, and to the development of 'radiations fields' (not addressed in this paper).

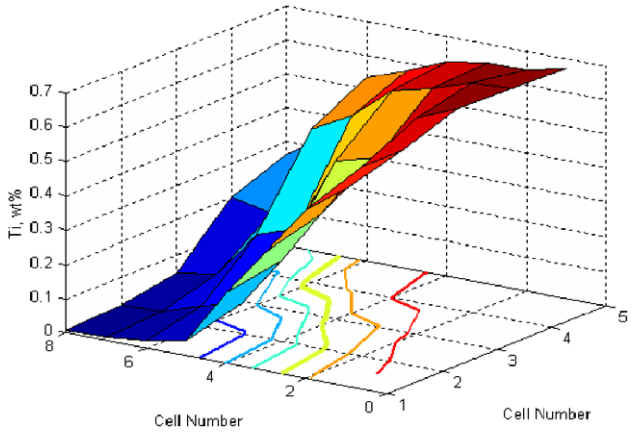

Fig. 27. Titanium contains % mean value for each trained cell (box) in the 8 × 5 Kohonen map. Titanium contained in Fe-based and Ni-based alloys increases the CGR.

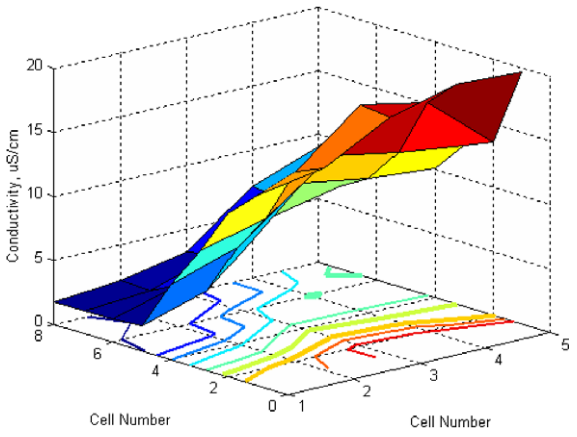

Fig. 30. Conductivity mean value for each trained cell (box) in the 8 × 5 Kohonen map. The environmental component of CGR is very dependent on the water conductivity. The Kohonen map captures this effect.

to the tip dissolution (oxidation)) encounters a larger area outside of the crack to be consumed. Fig. 30 supports this thesis. The reader is reminded that this result is obtained completely independently

of the conclusion reached by Macdonald by using a pure deterministic model to predict that CGRs – of thin cracks – increases with the flow rate of the electrolyte outside the crack [5,12]. This is the beauty of using data-mining techniques and comparing the results to existing theories.

3. Conclusion and recommendations

Stress corrosion cracking is one of the problems that can be presented in nuclear waste related system if metallic containers in wet environments are used. This paper presents, by first time, a methodology that is commonly used in data-mining techniques, and shows that this technique can be used successfully to establish relationship between important variables and crack grow rates. It is important to remember that the relationship discovered in between variables and stress corrosion cracking are not inclusive; i.e. they depend on the quality of the data measured. Dependence of stress corrosion cracking and other important variables may exist and they are not shown or discussed; because the data remained constant for those variables (for example, temperature, others).

It has been well established [4,5] that there is a close relationship between CGR and temperature, oxygen and hydrogen concentrations, and electrochemical potential. The data used in this work, for BWR environments, do not show any correlation between the CGR and those parameters (temperature, $[O_2]$, and ECP). The statistical analysis performed on the data showed a strong correlation between the 'mechanical' variables (K_{max}, ΔK_{max}, and ω) and the CGR; and a poor or non-existent correlation between the ECP and the electrolyte conductivity on the Fe-based alloys tested in BWR environments. The author concludes that these data are representative mainly (if not entirely) of the 'mechanical' regime and not of the 'environmental' or hydrogen 'embrittlement' regime.

When the Ni-based alloys in PWR environments data were mined, the results on the CGR obtained on the Kohonen clustering showed a lesser dependency on the 'mechanical' regime and a small dependency – or correlation – with 'environmental' variables, indicating that the data were collected in the transitional regime from 'mechanical' regime to 'environmental' regime.

This study enabled, through mining of the measured data, the gathering of information related to the regime under which the data were collected. This is very important, because it is essential that we be aware of prediction limitations, make extrapolations, and draw conclusions based on data that accurately represent the operational range of nuclear reactors. It is important to collect properly measured data in a wide, well-controlled-electrochemical-potential range that covers the phenomena that are observed in light water reactors.

This study also explores the impact of each one of the variables (alloy composition and the environment) on the CGRs. The author is not aware of any similar data mining techniques applied to nuclear reactors. The use of a similar methodology on a more general and larger data base is highly recommended.

Acknowledgement

The author would like to acknowledge the three reviewers for their insightful comments and corrections.

References

[1] O.K. Chopra, B. Alexandreanu, E.E. Gruber, R.S. Daum, W.J. Shack, Argonne National Laboratory, NUREG CR 6891-series ANL 04/20, Crack Growth Rates of Austenitic Stainless Steel Weld Heat Affected Zone in BWR Environments, January, 2006.
[2] B. Alexandreanu, O.K. Chopra, H.M. Chung, E.E. Gruber, W.K. Soppet, R.W. Strain, W.J. Shack, Environmentally Assisted Cracking in Light Water Reactors, vol. 34 in the NUREG/CR-4667 series annual report of Argonne National Laboratory program studies for Calendar (Annual Report 2003). Manuscript Completed: May 2005, Date Published: May 2006.
[3] B. Alexandreanu, O.K. Chopra, W.J. Shack, S. Crane, H.J. Gonzalez, NRC, Crack Growth Rates and Metallographic Examinations of Alloy 600 and Alloy 82/182 from Field Components and Laboratory Materials Tested in PWR Environments, NUREG/CR-6964, May 2008.
[4] D.D. Macdonald, M. Urquidi-Macdonald, in: D.D. Macdonald, Patrick Schmuki (Eds.), Appl. Electrochem., vol. 5, Wiley-VCH, Germany, 2006.
[5] Xinqiang Wu, Katada Yasuyuki, Corrosion Science ISSN 0010-938X CODEN CRRSAA 47 (6) (2005) 1415.
[6] T. Kohonen, Self-Organization and Associative Memory, second ed.., Springer-Verlag, Berlin, 1987.
[7] C.S. Kusko, J.N. Dupont, A.R. Marder, Weld. J. (2004). February.
[8] T.H. de Keijser, E.J. Mittemeijer, H.C.F. Rozendaal, J. Appl. Cryst. 16 (1983) 309.
[9] P. Marbelly, Contribution à l'étude des pics de diffraction Approche expérimentale et modélisation micromécanique, Thèse de Doctorat ENSAM Aix en Provence, 1996.
[10] K. Hirschi, Analyse des contraintes résiduelles et des paramètres microstructuraux par diffraction des neutrons dans un acier austénitique inoxydable, Thèse de Doctorat Université de Reims, 1999.
[11] Peter L. Andresen, Effects of Silicon on SCC of Stainless Steels and Alloy 182 Weld Metal, in: 12th International Conference on of Materials in Nuclear Power Systems-Water Reactors Environmental Degradation, Snowbird Resort Salt Lake City, Utah, USA American Nuclear Society, Refer to Gold File No. 57153207August 14–18, 2005.
[12] D.D. Macdonald, L.B. Kriksunov, Adv. Electrochem. Sci. Eng. 5 (1998) 125.
[13] M. Itatani, J. Fukakura, M. Asano, M. Kikuchi, N. Chujo, Nucl. Eng. Des. 153 (1994) 27.
[14] Digby D. Macdonald, Mirna Urquidi-Macdonald, Yingzi Chen, Jiahe Ai, Pilyeon Park, Han-Sang Kim, The Oxidation of Zircaloy Fuel Cladding in Water-Cooled Nuclear Reactors; Nuclear Energy Research Initiative (NERI) Final Report, Grant No. DE-FG03-02SF-22618, Final Report (September 15, 2002–September 14, 2006).